

Spectral Flow Cytometry Webinar Series

Watch our webinar series and learn how the ID7000™ system builds on Sony's experience with spectral analysis and simplifies many operations to advance the field of flow cytometry.



Watch Now

SONY



This information is current as of February 26, 2022.

RNA Splicing in the Transition from B Cells to Antibody-Secreting Cells: The Influences of ELL2, Small Nuclear RNA, and Endoplasmic Reticulum Stress

Ashley M. Nelson, Nolan T. Carew, Sage M. Smith and Christine Milcarek

J Immunol 2018; 201:3073-3083; Prepublished online 8 October 2018;
doi: 10.4049/jimmunol.1800557
<http://www.jimmunol.org/content/201/10/3073>

Supplementary Material <http://www.jimmunol.org/content/suppl/2018/10/05/jimmunol.1800557.DCSupplemental>

References This article **cites 44 articles**, 16 of which you can access for free at:
<http://www.jimmunol.org/content/201/10/3073.full#ref-list-1>

Why *The JI*? Submit online.

- **Rapid Reviews! 30 days*** from submission to initial decision
- **No Triage!** Every submission reviewed by practicing scientists
- **Fast Publication!** 4 weeks from acceptance to publication

**average*

Subscription Information about subscribing to *The Journal of Immunology* is online at:
<http://jimmunol.org/subscription>

Permissions Submit copyright permission requests at:
<http://www.aai.org/About/Publications/JI/copyright.html>

Email Alerts Receive free email-alerts when new articles cite this article. Sign up at:
<http://jimmunol.org/alerts>



RNA Splicing in the Transition from B Cells to Antibody-Secreting Cells: The Influences of ELL2, Small Nuclear RNA, and Endoplasmic Reticulum Stress

Ashley M. Nelson, Nolan T. Carew, Sage M. Smith, and Christine Milcarek

In the transition from B cells to Ab-secreting cells (ASCs) many genes are induced, such as ELL2, Irf4, Prdm1, Xbp1, whereas other mRNAs do not change in abundance. Nonetheless, using splicing array technology and mouse splenic B cells plus or minus LPS, we found that induced and “uninduced” genes can show large differences in splicing patterns between the cell stages, which could influence ASC development. We found that ~55% of these splicing changes depend on ELL2, a transcription elongation factor that influences expression levels and splicing patterns of ASC signature genes, genes in the cell-cycle and N-glycan biosynthesis and processing pathways, and the secretory versus membrane forms of the IgH mRNA. Some of these changes occur when ELL2 binds directly to the genes encoding those mRNAs, whereas some of the changes are indirect. To attempt to account for the changes that occur in RNA splicing before or without ELL2 induction, we examined the amount of the small nuclear RNA molecules and found that they were significantly decreased within 18 h of LPS stimulation and stayed low until 72 h. Correlating with this, at 18 h after LPS, endoplasmic reticulum stress and Ire1 phosphorylation are induced. Inhibiting the regulated Ire1-dependent mRNA decay with 4u8C correlates with the reduction in small nuclear RNA and changes in the normal splicing patterns at 18 h. Thus, we conclude that the RNA splicing patterns in ASCs are shaped early by endoplasmic reticulum stress and Ire1 phosphorylation and later by ELL2 induction. *The Journal of Immunology*, 2018, 201: 3073–3083.

The majority of multiexon containing mammalian genes are alternatively spliced, thereby producing on average four to five differently spliced products (1) with a large variation in proteins expressed (2). Alternative mRNA isoforms play important roles in normal development and physiology. Yet little is known beyond the IgH gene itself and the U1A small nuclear RNA (snRNA) protein expression about the overall landscape of alternative splicing and its effect on the path from B cells to Ab-secreting cells (ASCs). Upon stimulation by Ag, cytokines, or LPS, naive B cells drastically alter gene expression

to become ASCs (3). Thus far, RNA processing reactions have been implicated only in a small number of the changes seen in the differentiation to Ab secretion but are expected to play significant roles in others.

Extensive work from our laboratory (4) and that of others (5, 6) has shown that alternative 5' donor and 3' acceptor splice sites in the IgH μ gene are used in B cells, whereas in ASCs, the weak 5' splice site embedded in IgH μ CH4 is ignored to make secreted IgH μ mRNA and protein. Concomitantly there is a 10–100 fold increase in abundance of that mRNA over B cells because the RNA polymerase II (RNAPII) more efficiently transits the IgH μ gene and allows better recognition of the secretory-specific poly (A) site while engaging the highly induced transcription elongation factor ELL2 (11–19 lysine-rich leukemia gene), an important part of the super elongation complex (7–11). This led us to ask if ELL2 could influence the splicing of genes other than IgH in the B cell to ASC transition.

Meanwhile, we had also found a significant decrease in the amount of snRNA protein-associated U1A following stimulation to produce ASCs (12). This observation led us to ask if there were changes in the snRNAs that might also be involved in altering splicing when B cells differentiate into ASCs. Previous studies show that snRNAs could change splicing patterns, including during *Drosophila* development (13), in Alzheimer disease where the changed levels of U1 snRNA lead to altered RNA processing of several mRNAs (14), and in human diseases such as hematolymphoid neoplasia, retinitis pigmentosa, and microcephalic osteodysplastic primordial dwarfism type 1 associated with a loss of U4atac snRNA (15).

When B cells are stimulated to secrete Ab, the primary pathway for endoplasmic reticulum (ER) remodeling (also called the unfolded protein response; UPR) appears to uniquely include only the phosphorylation of inositol-requiring enzyme 1 α (Ire1) (16, 17) but not the Perk or Atf6 pathways seen in other cells. We had previously shown that mouse splenic B cells deficient in ELL2 are

Department of Immunology, University of Pittsburgh, Pittsburgh, PA 15261

ORCID: 0000-0002-3321-1694 (A.M.N.); 0000-0002-6995-6823 (N.T.C.); 0000-0002-3937-6828 (C.M.).

Received for publication April 24, 2018. Accepted for publication September 7, 2018.

This work was supported by AI124241 from the National Institutes of Health National Institute of Allergy and Infectious Diseases to C.M. and shared resources Grant P30CA047904 to the University of Pittsburgh Cancer Institute.

A.M.N., N.T.C., S.M.S., and C.M. performed the experiments and analyzed the data as well as helped write the manuscript and *Materials and Methods*. C.M. designed and supervised the study and wrote the manuscript with the assistance of the coauthors.

The microarray data presented in this article have been submitted to the Gene Expression Omnibus under accession numbers GSE113317, GSE113475, and GSE114435.

Address correspondence and reprint requests to Dr. Christine Milcarek, Department of Immunology, University of Pittsburgh, Room E1059 Biomedical Science Tower, Terrace and Lothrop Streets, Pittsburgh, PA 15261. E-mail address: milcarek@pitt.edu

The online version of this article contains supplemental material.

Abbreviations used in this article: ASC, Ab-secreting cell; ChIP, chromatin immunoprecipitation; ChIP-seq, ChIP sequencing; cKO, conditional knockout; ER, endoplasmic reticulum; GEO, Gene Expression Omnibus; Ire1, inositol-requiring enzyme 1 α ; NCBI, National Center for Biotechnology Information; QPCR, quantitative PCR; RIDD, regulated Ire1-dependent mRNA decay; RNAPII, RNA polymerase II; snRNA, small nuclear RNA; TAC, Transcriptome Analysis Console; UPR, unfolded protein response; UTR, untranslated region.

Copyright © 2018 by The American Association of Immunologists, Inc. 0022-1767/18/\$37.50

www.jimmunol.org/cgi/doi/10.4049/jimmunol.1800557

unable to secrete Ig after LPS stimulation but still maintain Ire1 phosphorylation, an ER stress sensor (9). Interestingly, the phosphorylation of Ire1 occurs even when IgH μ secretion is rendered moot by mutations in the IgH μ gene itself and in the activation-induced cytidine deaminase AID/Aicda gene to prevent subclass switching (18). Therefore, much of the ER stress that occurs in B cell activation precedes Ig secretion. The phosphorylation of Ire1 results in acquisition of a regulated Ire1-dependent mRNA decay (RIDD) (19, 20). We wondered if this pathway could play a role in the stark transcriptional divide between B cells and ASCs and influence splicing patterns in some way.

In this study, we analyzed the changes in splicing between resting primary splenic mouse B cells and their resultant LPS-stimulated ASCs. We sought to understand the forces which could alter the splicing patterns. We compared splicing patterns in B cell conditional knockouts (cKOs) of ELL2 with ELL2-positive litter mates and found that some, but not all, of the changes in alternative splicing were altered by eliminating that induced elongation factor. We explored what else might be responsible for the altered splicing. We found that the levels of all the classical and noncanonical (AT/AC) RNAPII transcribed snRNAs were reduced following LPS stimulation. Eliminating the RIDD activity of Ire1 changed snRNA levels and changed splicing patterns. Overall, ER stress and ELL2 induction contribute to the changes seen in RNA splicing in the development of ASCs.

Materials and Methods

Affymetrix Clariom D RNA microarray and analysis

RNA samples from at least three independent biological samples were obtained as described below and sent to the University of Pittsburgh Genomics Research Core, where the Affymetrix array was performed. Analysis of the data was performed using Transcriptome Analysis Console (TAC) software from Affymetrix. Samples were analyzed using default parameters. An alternative splicing event was defined as a differentially expressed exon with at least a 2-fold change in expression, at a p value of $p = 0.05$ or better. The TAC software was set to identify the change in exon expression as one of the five classifications for alternative splicing based on the expression patterns of the surrounding exons. For gene enrichment analysis, gene lists were submitted to the ConsensusPathDB Web site developed by the Max Planck Institute for Molecular Genetics. Overrepresentation analysis returned pathway-based set results. The most enriched pathways were grouped and tabulated.

Mice

The derivation and characterization of the ELL2 loxp/loxp exon3 mice crossed with the C57BL/6 CD19cre mice (no. 006785; The Jackson Laboratory) to inhibit Ig secretion was described previously (9). Naive splenic B cells were extracted from those mice that had been crossed with either CD19^{+/+} (designated wild type littermates) or CD19^{+/cre} (exhibiting a cKO of exon 3 in the ELL2 gene). Deletion of the exon 3 of ELL2 in cre⁺ mice in LPS-stimulated B cells and reduction in IgH secretory mRNA were verified by a real-time PCR assay with the DNA and mRNA, respectively. All mice were maintained at the University of Pittsburgh animal facilities, and experiments were undertaken and conducted in accordance with institutional policies as per Animal Welfare Assurance number A3187-01. The ELL2 exon 3 loxp/loxp mice have been deposited at The Jackson Laboratory as stock no. 029528 and are available for unrestricted use.

B cell isolation and stimulation

Naive splenic B cells were extracted from 6- to 20-wk-old ELL2 loxp/loxp exon 3 mice, with either CD19^{+/+} or CD19^{+/cre}, and isolated using the autoMACS system (no. 130-090-862; Miltenyi Biotec) as previously described (9). The cells were cultured in medium on day 0 at 5×10^6 cells/ml. The cells were counted via hemocytometer, split, and cultured at 1×10^6 cells/ml for up to 72 h with LPS at 20 μ g/ml in RPMI 1640 medium containing 50 μ M 2-ME, 2 mM glutamine, 10% FBS, 1 mM sodium pyruvate, nonessential amino acids, 1 \times penicillin/streptomycin, and 1 mM HEPES buffer. CD138⁺ cells were isolated using CD138 MACS MicroBeads from Miltenyi Biotec (Cat. no 130-098-257) as per the manufacturer's instructions.

Chromatin immunoprecipitation sequencing and chromatin immunoprecipitation quantitative PCR

Chromatin immunoprecipitation (ChIP) sequencing (ChIP-seq) arrays were performed by Active Motif (Carlsbad, CA). DNA was prepared for amplification by converting overhangs into phosphorylated blunt ends and adding an adenine to the 3' ends. Illumina genomic adapters were ligated, and the sample was size fractionated (200–300 bp) on an agarose gel. After a final PCR amplification step (18 cycles), the resulting DNA libraries were quantified and sequenced on HiSeq 2000. Sequences (50 nt reads, single end) were aligned to the mouse genome (mm10) using the Burrows–Wheeler algorithm. Alignments were extended in silico at their 3' ends to a length of 150 bp. Active Motif used their proprietary software to analyze the data. More than 17 million reads were obtained, and peaks were called using the MACS (v.1.4.2) algorithm, with a cutoff p value of $p = 0.00005$. Reads were aligned to the mouse genome (mm10) and visualized in the Integrated Genome Browser (University of California, Santa Cruz, Santa Cruz, CA). The anti-ELL2 mouse polyclonal anti-peptide Ab 4502 (10) was used in triplicate for the positive signal and compared with a control nonspecific rabbit Ab with the AxJ mouse plasma cell line (IgG2a, k, λ) we have studied extensively (7). The AxJ cells were verified by sequencing the H chain V region. Confirmation of a portion of the ChIP-seq data were performed with conventional ChIPs as previously described (9), using the quantitative PCR (QPCR) probes in the list of primers in Supplemental Table I.

IRE1 inhibitor treatments

Primary splenic B cells were treated with Ire1 ribonuclease inhibitor 4 μ 8c (Sigma-Aldrich) at a concentration of 5 μ M (21) in DMSO in the presence of LPS, as described above. Samples were taken at 0, 6, 18, and 24 h. The 18-h samples were used for the array and western data. Control cells were treated with equivalent amount of DMSO and taken at the same time points.

RNA isolation and quantitative RT-QPCR

RNA was isolated from cells using the RNeasy Mini Kit (no. 74106; Qiagen) or Macherey-Nagel NucleoSpin RNA/Protein kit (Cat. no. 740933). RNA was copied using SuperScript First-Strand Synthesis for RT-QPCR following the random oligonucleotide procedure (no. 11904-018; Invitrogen). Quantification by QPCR was performed using Sybr Green PCR Master Mix (no. 4909155; Applied Biosystems) along with the identified primers (Supplemental Table I). The instrument used was a StepOnePlus Real-time QPCR System from Applied Biosystems. The cycle quantification time values were normalized as log fold change relative Hprt as a constant, and GraphPad Prism 7 software was used for graphing and statistical analyses. B cell and Go values were normalized to 100.

Statistics

Data are shown with SEM error bars, and significance is calculated using GraphPad Prism 7 software with a two-way ANOVA such that $*p < 0.05$, $**p < 0.01$, $***p < 0.001$, and $****p < 0.0001$. Experiments in Figs. 1B, 2A, 2C, 4B, 5, and 6 were performed at least three times with at least three independent biological samples. We used Hprt, Gapdh, and Actb mRNAs as internal controls; the level of Hprt mRNA was previously shown to remain constant through LPS stimulation of B cells (22, 23).

Western blotting

Protein samples were obtained from whole cell extracts that were sonicated briefly to reduce viscosity. Western protocol from the Bio-Rad Laboratories General Protocol (Bulletin 6376 Rev A) was followed. Molecular weight markers were the Precision Protein Kaleidoscope markers from Bio-Rad Laboratories (no. 161-0375). Bio-Rad Laboratories Mini-PROTEAN precast gels were used. Abs used include anti-Ire1 Abcam no. 37073, anti-Ire1ser724P from Thermo Fisher Scientific PA1-16927 (Invitrogen), anti-SnapC/43 kDa (k-16; sc20241) goat polyclonal from Santa Cruz Biotechnology, and other primary and secondary Abs as previously described (9).

Availability of the data

The ChIP-seq and Affymetrix splicing array data have been deposited at the National Center for Biotechnology Information (NCBI) Gene Expression Omnibus (GEO) (GSE 113317, GSE113475, and GSE114435) publicly available web sites. Affymetrix splicing array data accession no. GSE113317 deposited on April 18, 2018, for plus or minus LPS 72 h and plus or minus ELL2 is viewable at <https://www.ncbi.nlm.nih.gov/geo/query/acc.cgi?acc=GSE113317>. Microarray data no. GSE 113475 for the 0 and 18 h LPS plus or minus 4u8C, deposited on April 21, 2018, is viewable at <https://www.ncbi.nlm.nih.gov/geo/query/acc.cgi?acc=GSE113475>. Raw data for

ChIP-seq data (GSE114435) is deposited and viewable at <https://www.ncbi.nlm.nih.gov/geo/query/acc.cgi?acc=GSE114435>. The data for ChIP-seq are associated with Fig. 4 and Supplemental Table II. Affymetrix splicing data are associated with Figs. 1–3 and 7 and Supplemental Table II. There are no restrictions on the availability of the datasets.

Results

Major splicing changes occur when B cells become ASCs

Although it is well known that there are changes in the genes expressed between B cells and ASCs, we wanted to determine if overall splicing changes were also occurring. We used splicing arrays and the TAC software from Affymetrix to answer this question. These arrays enable one to assess the differences in overall expression levels as well as alternative splicing of individual mRNAs. First we validated the differentiation of our samples from B cells into ASCs by 72 h of LPS stimulation by observing their increased IgH secretory mRNA, ELL2 mRNA production, and CD138 surface protein acquisition by QPCR and flow cytometry; these RNA changes in expression were also seen in the array data. In addition, in the data we obtained and deposited at the NCBI GEO site, we noted that many key genes are induced to higher expression levels in the transition after 72 h of LPS treatment to the ASCs, like *Irf4*, *blimp1* (*Prdm1*) and the ASC “signature genes” previously described (3). Meanwhile, many other genes do not change mRNA abundance; nonetheless, we noted that they change their splicing patterns. We show the splicing tracks for three such genes in which mRNA abundance does not change, but splicing does (Fig. 1A); orange means that an exon is enriched in B cells, whereas blue means it is enriched in ASCs. The more intense the color the larger the enrichment. These genes have been reported to have mRNA isoforms that can encode different proteins based on the splicing alterations. For example, histone deacetylase 9 (*Hdac9*), which is missing exon 7, is reported to be retained in the cytoplasm, whereas proteins encoded by mRNA with exon 7 (dark blue), enriched here in ASCs, are reported to enter the nucleus to acetylate histones to activate gene transcription (24). Polypyrimidine track binding protein 3 (*Ptbp3*) is an RNA binding protein that mediates precursor mRNA alternative splicing. Exon 2 inclusion (seen here in orange), previously shown to be enriched in B cells, is known to result in greater nuclear localization and an extra RNA binding domain (25). As shown in this article, forms without exon 2 are enriched in ASCs. *MyD88*, a universal adapter protein used by almost all TLRs (except TLR 3) to transmit signals and activate the transcription factor NF- κ B, has been shown to exist in a long form (with the orange retained intron) that activates immunity, whereas the short form, without the intron, inhibits TLR signals and usually arises after LPS treatment (26, 27). We see these short forms after 72 h of LPS stimulation. Fig. 1B validates the splicing array differences by QPCR for *MyD88*. The array results for several other genes were also validated by QPCR (data not shown). Thus, changing splicing patterns can influence mRNA function, and in the examples illustrated, the changed splicing patterns were shown to generate alternative forms of the protein. We saw changes in the splicing patterns when comparing B cells to ASCs (plus LPS for 72 h) in other genes that have previously been reported to be capable of producing different isoforms of mRNA and protein. Among those genes in which the splicing patterns are changed at least 3-fold after 72 h of LPS in our microarray studies (see GEO data) are the following: *Traf7*, *Zbtb20*, *DNAJB6* (*hsp40*), *IL-2R* γ -chain, *Ppp2r5c*, *Srsf1*, *Ikzf1*, *Cmp1* (*c-maf*), *Elmo*, *Ugp2*, *Picalm*, *Tmem209*, *Hspa4* (*hsp70*), *Mapk1*, *Xiap*, *Eifak3*, *Cstf3*, and *Srpk2*. We have not pursued potential changes in protein expression by mass spectros-

copy analyses for these, but the finding that these genes could be encoding alternative protein forms provides insight into the potential importance of altered RNA splicing during the B cell to ASC transition.

In the totality of mRNA coding genes that were expressed in both B cells and ASCs at 72 h, many have different splicing patterns that have not yet been shown to result in different protein isoforms. There are 9326 genes that show RNA splicing differences in the two conditions, as summarized in Fig. 1C; note, some genes may have several types of splicing alterations, so there are many more changes on summing the events than the total number of genes involved. The majority of genes with altered splicing show changes in a “Cassette Exon” event (6533), which denotes the inclusion or skipping of a single exon in an mRNA isoform. Because there are 16,411 exons included or skipped in 6533 genes where this happens, there are roughly 2.5 of these changes per gene. This is a remarkable number of changes. Uses of alternative 5' donor and 3' splice acceptor sites are the next most common alternative splicing events. Intron retention can occur as well, with mutually exclusive exon usage occurring, but less frequently than the rest (0.7%). The enormity of the changes we see in B cells versus ASCs at 72 h after LPS indicates that the splicing landscape is significantly different between the two.

Loss of ELL2 changes gene expression levels in ASCs

Although numerous splicing changes that were heretofore unappreciated could significantly impact the gene expression profile of ASCs, we focused not on the consequence of all those changes but rather on how these changes in the splicing milieu of the cells are brought about. Because transcription elongation rate and alternative splicing had been previously linked (28), we first hypothesized that based on its role as a transcription elongation factor, ELL2 might have a significant role in changing the landscape of alternative splicing in ASCs. We examined global changes in mRNA levels that might accompany loss of ELL2. As shown in Fig. 2A, when the ELL2-sufficient splenic B cells were stimulated with LPS for 72 h they produced 25-fold more of the secreted form of Ig μ H chain versus the membrane-specific form. Meanwhile, ELL2-deficient cells (cKO Fig. 2A) were impaired in the production of the secretory specific form as we had previously shown (9, 29). ELL2 induction is also impaired in the cKO cells. These were the samples used for our subsequent analyses. In data not shown, we found that ELL2 is not significantly induced until 24 to 36 h after LPS treatment of B cells.

We assessed global expression after 72 h of LPS stimulation of splenic B cells, and, as shown in Fig. 2B (upper left and right quadrants), in the plus versus minus ELL2, a large number of genes (>1000) are altered in their abundance. The majority show decreased levels in the absence of ELL2. Of these, 192 were V region genes for heavy or light Ig chains. A complete list of the 851 non-V regions induced by ELL2 is shown in Supplemental Table II whereas the complete data set is deposited at the NCBI GEO Web site. ELL2 induction therefore has a broad effect on mRNA abundance in ASCs at 72 h post LPS.

Among the genes whose mRNA abundances are increased when ELL2 is present, we concentrated first on 48 signature ASC genes described as expressed at higher levels after all modes of stimulation to produce ASCs by Shi et al. (3); *Irf4* and *Prdm1* (*blimp1*) are included for completion. As shown in Fig. 2C, a positive fold-change value is shown for the majority of the signature genes indicating higher levels of expression in the ELL2^{+/+} than the ELL2 cKO cells. There are just three exceptions. These data show that ELL2 has a major impact on the expression of the signature ASC genes, as well as *Irf4* and *Prdm1*.

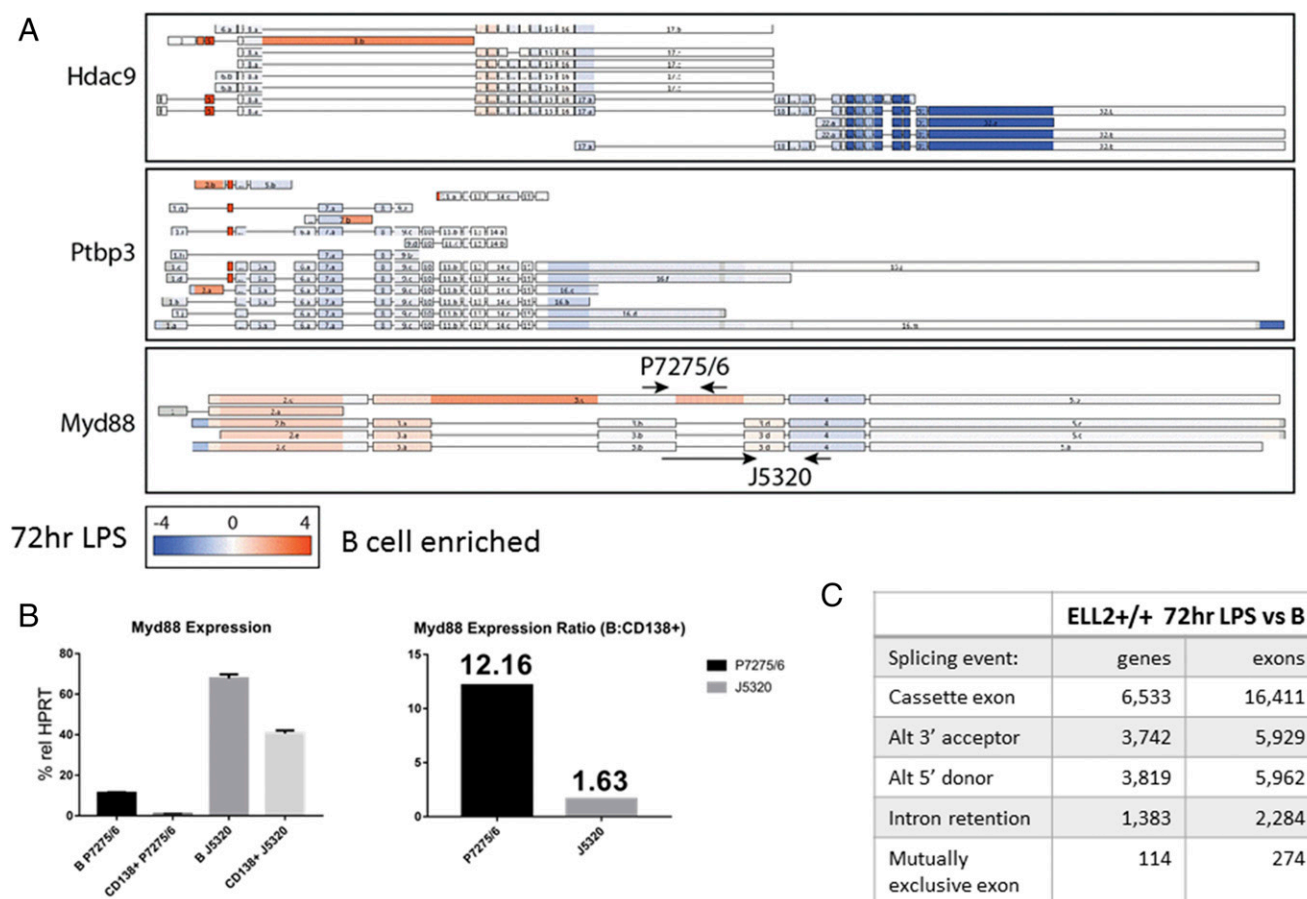


FIGURE 1. Major splicing changes occur when B cells become ASCs. **(A)** TAC software analysis of alternative splicing tracks of B cell example genes before and after LPS. The overall abundance of these sample mRNAs in this panel did not change. B cell (–LPS) splicing enrichment is indicated by orange, and +LPS enrichment is represented by blue, with the intensity of the color corresponding to fold change in expression of that region of mRNA, depicted by the scale at the bottom. The indicated P7275/6 forward primer is in the standard exon, whereas the reverse is in the retained intron. The J5320 forward primer spans the junction between section 3b and 3d, whereas the reverse sits downstream in an exon. **(B)** *Myd88* expression levels with validation primers in **(A)** relative to *Hprt* and RT-QPCR are shown. The expression ratios (B/CD138⁺) of validation primers between the unstimulated B cells and stimulated CD138⁺ cells. Three independent biological samples were used with triplicate determinations in the QPCRs. **(C)** TAC software classifiers for differentially spliced events, broken down by number of genes and number of exons in each class. Comparison in ELL2^{+/+} cells in B cells versus LPS-stimulated ASCs. Results determined by averaging five independent biological replicates for the array data, see *Materials and Methods*.

ELL2 impacts alternative splicing

We then asked how ELL2 would change the landscape of alternative splicing. The ASC signature genes marked with an asterisk (*) in Fig. 2C show alternative splicing with ELL2 in the microarray studies (45 of 52) and are listed as such in Supplemental Table II with the other ELL2 induced genes. A few examples of alternative splicing TAC patterns of nonsignature genes, also listed in Supplemental Table II, are shown in Fig. 3A to indicate the specific ELL2-dependent changes in splicing patterns. These three have mRNAs isoforms with more abundant, extended 5' untranslated regions (UTRs) when ELL2 is knocked out (orange). Longer 5' UTRs have been shown to lead to mRNAs, bearing them to be less effectively translated (30). Thus, when ELL2 is absent, the 5' end of the mRNA is retained more often. The splicing pattern of ELL2 mRNA itself is shown in Fig. 3A; when comparing the wild type (blue) to the knockout cells, exon 3 is much more abundant in the wild type because this is the exon flanked by loxP sites in the cKO.

Extending beyond the 851 ELL2-induced genes, we next turned to the global splicing profile in cells 72 h after LPS when ELL2 is missing, summarized in Fig. 3B. We see that the number of genes affected by differential splicing events in cells stimulated by LPS

for 72 h in ELL2-deficient cells is significantly reduced in all categories relative to when ELL2 is present (Fig. 3B); there are only 5256 genes affected and there are fewer multiple splicing events per gene. Loss of ELL2 results in many changes in all the splicing types (cassette, 3' acceptor, 5' donor, intron retention, mutually exclusive exons); compare Fig. 3B with the ELL2-sufficient cells in Fig. 1C. Proportionally, the mutually exclusive exon category is most impacted by the loss of ELL2 (down to 0.2%). To understand how much of the alternative splicing in ELL2-sufficient cells at 72 h requires the action of ELL2, we created the Venn diagram (Fig. 3C). It shows that mRNA from 9326 genes is alternatively spliced in cells 72 h after LPS addition when ELL2 is present, but among these, only 4211 are alternatively spliced when ELL2 is absent. Thus, we conclude that significantly more than half of the 9326 genes (that is, the remaining 5115) require ELL2 to be present to have the proper alternative splicing occur.

ELL2 binds to many genes for elongation

Next, we asked which mRNAs have genes that are direct targets of ELL2. To address this, we performed ChIP-seq experiments using Ab to ELL2. We previously showed that ELL2 is found on

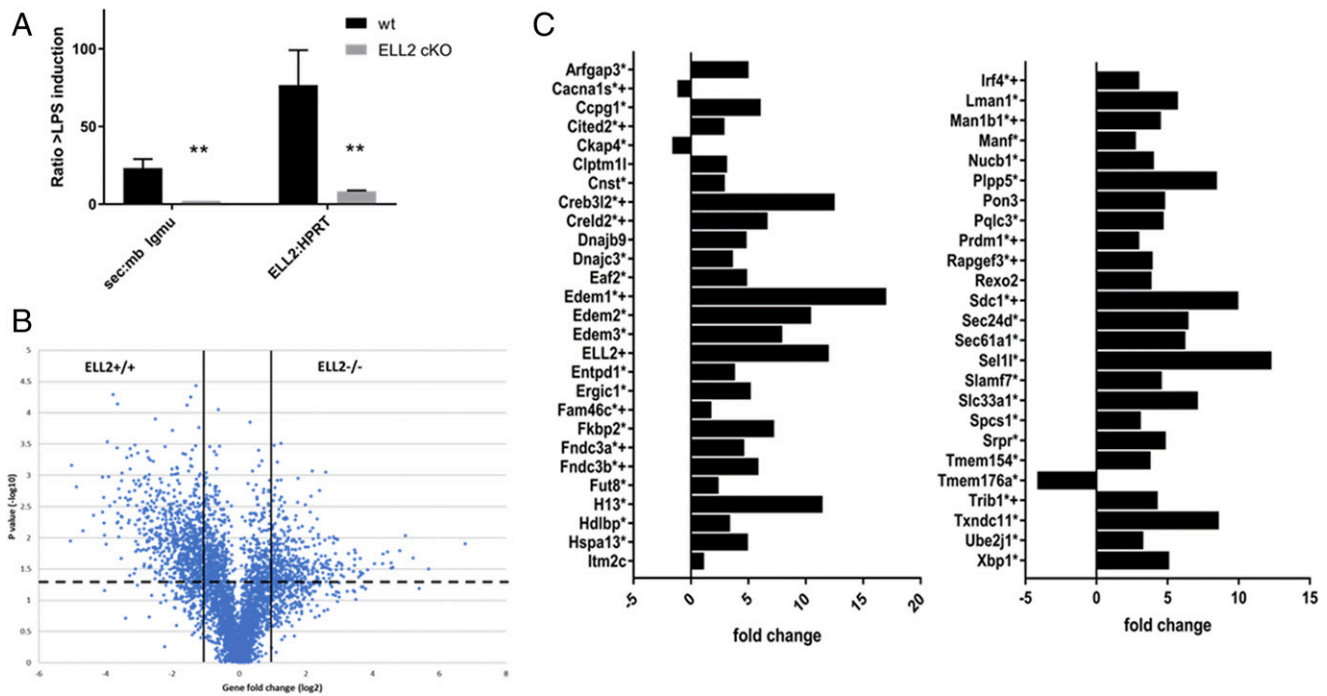


FIGURE 2. Loss of ELL2 changes gene expression levels in ASCs. **(A)** mRNA levels in splenic B cells plus or minus ex vivo LPS for 72 h. The ELL2 cKO mice are ELL2 loxp/loxp CD19cre/+ and the wild type (wt) are their ELL2+/+ litter mates. RNA was converted to cDNA, and real-time PCR was conducted using the secretory-specific or membrane-specific probes for Igmu H chain or a probe for exon 3 of ELL2 normalized to Hprt. Error bars indicate SEM. ***p* = 0.01 from three independent biological replicates and triplicate QPCRs. **(B)** mRNA levels in LPS-stimulated ELL2+/+ and ELL2-/- (cKO) cells 72 h after LPS addition. Genes are named in Supplemental Table II. Dashed line indicates *p* = 0.05 (ANOVA), solid lines show linear fold change of ± 2. **(C)** Expression profile changes in 48 signature ASC genes, plus Prdm1 and Irf4. Bars represent the linear fold change in expression of each gene, with positive fold-change values indicating higher levels in the ELL2+/+ than the ELL2-/- cKO cells. Error bars are omitted for clarity. + indicates that the gene binds ELL2 in ChIP. * indicates genes that mRNAs are alternatively spliced after LPS stimulation in ELL2+/+ cells. Three independent biological samples were used for each type of mouse, and QPCRs were performed in triplicate. ***p* < 0.01.

chromatin with RNAPII through its association with the super elongation complex (10, 31). ChIP was performed on a mouse plasma cell line, and the products were subjected to deep sequencing and analysis with the help of Active Motif and ChIP-IT software. There are ~2000 candidates with >10 tags per peak. Genes that bind ELL2 and that also show increased abundance in the presence of ELL2 are shown in Supplemental Table II. The complete data set of 2000 ELL2 ChIP targets is deposited at the NCBI GEO Web site. ELL2 protein binds to a number of highly expressed genes, including *Atf6*, *Pou2af1* (*OcaB*, *Bob1*, *Obf1*), several heat shock genes, IgH enhancers (both near the μ C region [IgH Emu] and downstream of the IgH α genes [IgH Ealpha]), IgH C regions, Ig H and L chain genes, *Prdm1* (*blimp1*), *Irf4*, several ASC signature genes, and *Mdm2*. The tracks of the ELL2 protein on several of the genes are shown in Fig. 4A. In the tracks, ELL2 is often associated strongly with the region near the promoter where RNAPII is found in abundance on an active gene. The results from the ChIP-seq were confirmed using standard ChIP QPCR on several of the genes as shown in Fig. 4B, using LPS-stimulated primary splenic B cells that were harvested 72 h after LPS stimulation and selected as CD138+ (i.e., ASCs). Therefore, the changes in splicing expression of some genes we see are a direct result of ELL2 association after induction; meanwhile, some changes after ELL2 induction are indirect. Some ASC signature genes shown in Fig. 2C are direct targets of ELL2 (indicated by a + sign in that figure) along with more of the upregulated RNAs shown in the ELL2+/+ area in Fig. 2B (see Supplemental Table II).

A pathway analysis (Fig. 4C) of 343 of the ELL2 direct targets (from ChIP-seq) that are also induced in expression and are most

highly alternatively spliced as shown in this study indicates that the genes are in eight cell cycle pathways, six N-glycan biosynthesis and processing pathways, four immune signaling pathways, four in Golgi pathways, and five in protein processing in the ER. ELL2 binds to genes in these pathways, increases the abundance of their mRNAs, and changes their splicing patterns.

snRNA expression decreases after LPS stimulation

Having previously seen changes in U1A expression after stimulation of B cells to ASC (12), we wondered if the small RNAs themselves, which directly participate in splicing, are influencing and perhaps influenced by the differentiation of B cells to ASCs. Changing the level of the snRNAs might contribute to the additional splicing changes seen in this study as it has in the examples cited in the introduction. Splicing arrays and several other mRNA deep sequencing techniques underrepresent the snRNAs, so we used RT-QPCR to investigate their amounts.

We examined the levels of the snRNAs before and after 72 h of LPS treatment of mouse splenic B cells by making cDNA using random primers and then using RT-QPCR with U snRNA gene-specific primers. As shown in Fig. 5A, the levels of most of the small RNAs falls off in cells treated with LPS for 72 h (ASCs) relative to B cells, set as 100% to normalize for the different basal levels of expression, with the levels of most of the Uatac snRNAs (U11, U4atac, U6atac) falling to <10% of that seen in B cells. The U6 snRNA gene is transcribed by RNAPIII, in contrast to the others (32).

Next, we investigated whether the low levels of the Uatac snRNAs in particular might correlate with the expression of some genes known to contain the AT/AC style introns, such as U1A,

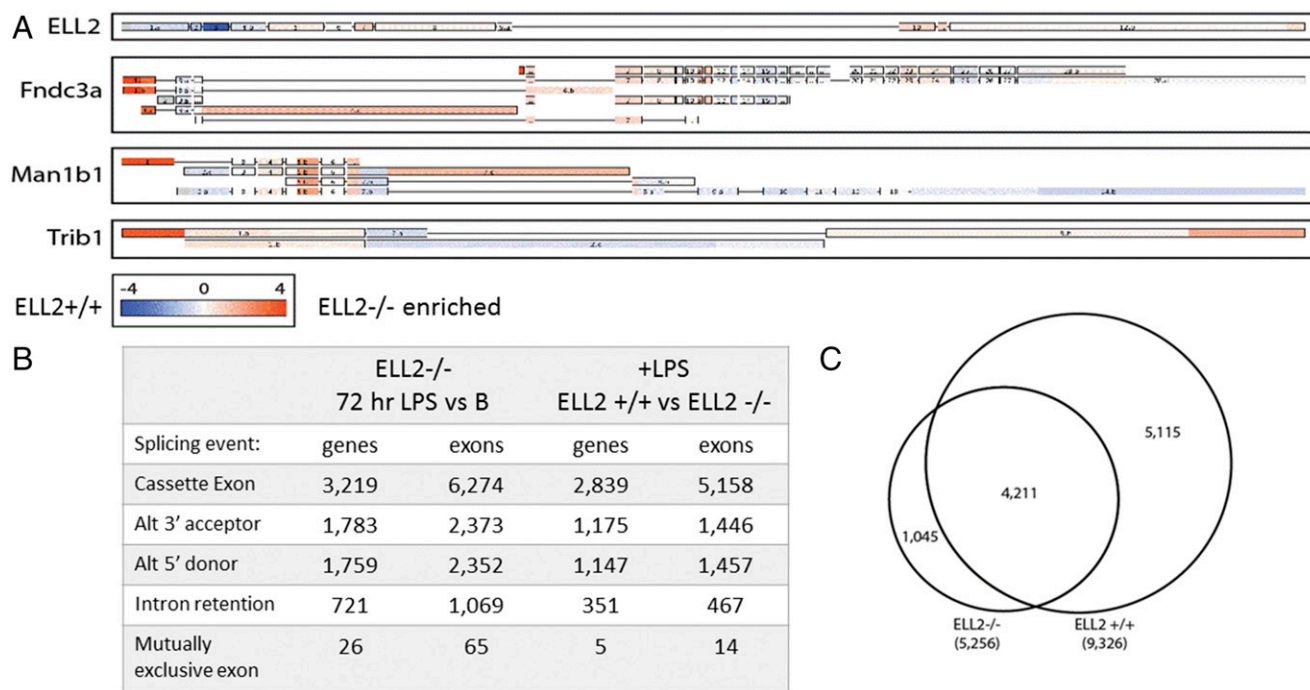


FIGURE 3. ELL2 impacts alternative splicing. **(A)** TAC software generated splicing tracks of selected ASC signature genes comparing stimulated ELL2-sufficient and -deficient cells. ELL2^{+/+} enrichment is indicated by blue, ELL2 cKO enrichment is represented by orange, with the intensity of the color corresponding to fold change in expression and depicted by the scale at the bottom. **(B)** TAC software classifiers for differentially spliced events, broken down by number of genes and number of exons. Comparison of ELL2^{-/-} cells plus LPS for 72 h versus B cells and 72 h LPS-stimulated cells comparing ELL2^{+/+} versus ELL2 cKO. At least three independent biological samples were used for each genotype of mouse for the array data. **(C)** Venn diagram depicting the amount of overlap between alternatively spliced genes (B cells versus 72 h plus LPS) in the ELL2^{+/+} and ELL2 cKO data sets.

HnmpLL, and Ints10. As shown in Fig. 5B, the level of these mRNAs was significantly reduced after 72 h of LPS. Other genes with AT/AC introns, such as Fyn, were previously shown to decrease in ASCs (33, 34). When U4atac is mutated in humans, a condition called microcephalic osteodysplastic primordial dwarfism type 1 results, and AT/AC introns are not properly spliced (35). This suggests that the drop we see in U snRNAs between splenic B cells and ASCs could influence the splicing of some AT/AC intron-containing genes and perhaps other genes as well, either directly or indirectly.

We examined the levels of the mRNA encoding some of the snRNA transcription factors. The transcription of snRNAs requires cooperative binding of five SnapC subunit proteins with Oct1 (and or Oct2) to the octamer sequence for each of the snRNA enhancers (36, 37). A little elongation complex including Ice1 and Zc3h8 with ELL1 forms and travels with RNAPII to synthesize the snRNAs (38). The Integrator complex of at least five proteins is necessary for snRNA transcription termination. We showed that the mRNA for the Ints10 gene is decreased in Fig. 5B, and in Fig. 5C we show that the levels of mRNA for SnapC1 and SnapC2 are also decreased. This is also true for the SnapC1 43 kDa subunit protein, as shown in Fig. 5D.

Loss of snRNAs occurs early with ER stress

The data indicate a marked drop off of snRNAs between B cells and cells treated with LPS for 72 h. We did a time course of expression of the U RNAs and saw that the drop off begins within 18 h of LPS treatment (Fig. 6A) before ELL2 is induced, which occurs around 24–36 h. We also examined the relative loss of the small RNAs in blimp1 (Prdm1) knockout mice and saw a reduction similar to that seen in blimp1⁺ mice (data not shown). Thus, the changes start early and seem to be Prdm1/blimp1 independent.

It seemed possible that the decrease in snRNA levels could be attributed to decreases in the SnapC mRNAs that we saw, the ER stress induced by LPS treatment, and/or the Ire1-linked RIDD pathway (20). The phosphorylation of Ire1 is apparent by 18 and 24 h after LPS treatment and also at 72 h (see Figs. 5D and 6B), and as expected, Xbp1 expression and the short form of Xbp1 increase with time after LPS. Meanwhile, SnapC1 (Snap43) protein is decreased by 18 h, similar to its mRNA.

To determine if the decrease in SnapC1 and 2 might be correlated with the RIDD activity of Ire1, we cultured primary splenic B cells stimulated for 18 h with LPS plus and minus the RIDD inhibitor, 4μ8c (21). With 18 h of LPS, the splicing of Xbp1 to create the short form of the protein is increased, indicating that RIDD is active; but in LPS plus the inhibitor 4u8C, there is little to no Xbp1 splicing (Fig. 6). The analysis of the Ire1 protein showed that its autophosphorylation was occurring without 4u8C but not in its presence (Fig. 6B). Meanwhile, at 18 h with LPS and no inhibitor, the SnapC1 mRNA is decreased, whereas in the presence of the drug there is a significant increase in its level. Likewise, in LPS and with no 4u8c, the U1 and U11 snRNA levels are slightly decreased at 18 h, whereas the addition of the RIDD inhibitor dramatically increases their amount (Fig. 6A). Altering the snRNA content in the cell could cause changes in expression of other regulators such as U1A, HnmpLL and Ints10 and could thus contribute to the altered splicing patterns in ASCs.

ER stress influences splicing patterns

Next we sought to determine if the ER stress response was accompanied by alterations in the B cell splicing patterns at 18 h post-LPS. The Affymetrix splicing arrays were used to analyze splenic B cell samples at time 0 and 18 h after LPS stimulation, plus and minus 4u8C, the drug shown above to influence the RIDD activity of Ire1-P (21). We compiled the differential splicing events and

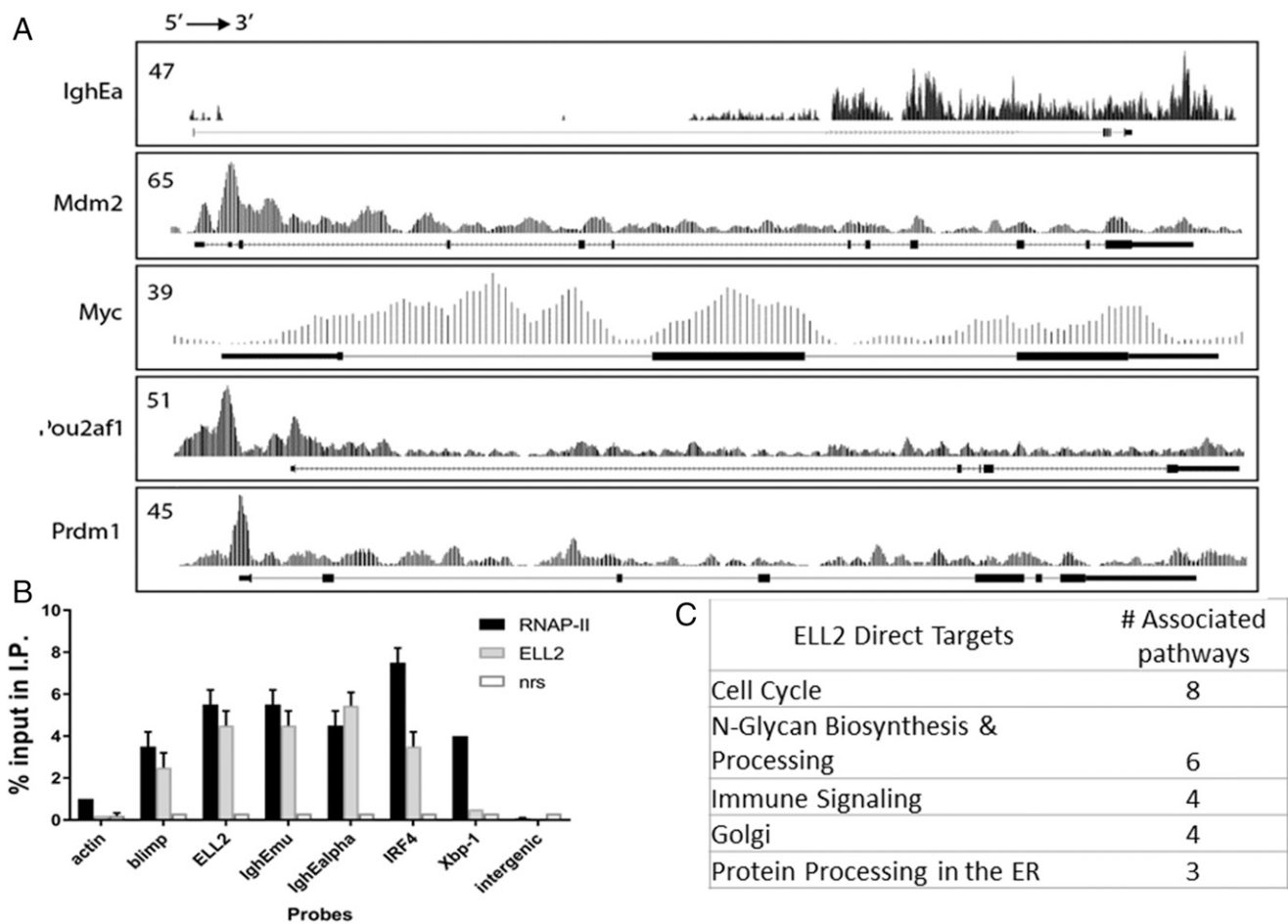


FIGURE 4. ELL2 binds to many genes. **(A)** ChIP-seq tracks of ELL2 on the IgH enhancer α region, along with other genes of interest. Track numbers on the left indicate the highest number of tags per peak. mRNA coding region of each gene is shown below the tracks, exons in dark boxes. Direct targets of ELL2 with an influence on mRNA abundance and or splicing are enumerated in Supplemental Table II. **(B)** ChIP analysis of LPS-stimulated ASC chromatin from ELL2^{+/+} immunoprecipitated with Ab to RNAPII or ELL2. Normal rabbit anti-sera (nrs) is a control. Immunoprecipitated (I.P.) DNA was analyzed by real-time PCR relative to the input sample taken before the ChIP steps. At least three independent biological replicates were used for ChIP, and the QPCRs were performed in triplicate. **(C)** Tally of pathway analyses of 343 alternatively spliced ELL2 direct targets by ChIP that are also alternatively spliced between the ELL2^{+/+} and ELL2 cKO plus LPS, with $p = 0.001$.

report them in Fig. 7A and on the NCBI GEO Web site. Blocking the RIDD function of Ire1-P by 4u8C was correlated with significantly reduced overall number of splicing events in mRNA in all categories. Mutually exclusive exon splicing, in particular, was reduced by 3-fold. The number of genes that were alternatively spliced was reduced from 11,144 without inhibitor to 7248 with the 4u8C inhibitor.

When we cross referenced the 4211 genes that are alternatively spliced at 72 h of LPS regardless of ELL2, the ELL2-independent genes, with the 0–18 h family of alternatively spliced genes, we see that many of the ELL2-independent genes (~90%, 3783 of 4211) are included in the 0–18 h group (Fig. 7B). Thus, they change early and before ELL2 is induced, as we predicted. We conclude that many splicing changes occur before ELL2 is induced, but while RIDD is activated and U snRNA levels are falling, some of these alternative splicing events persist until the 72 h plus LPS stage, whereas others do not.

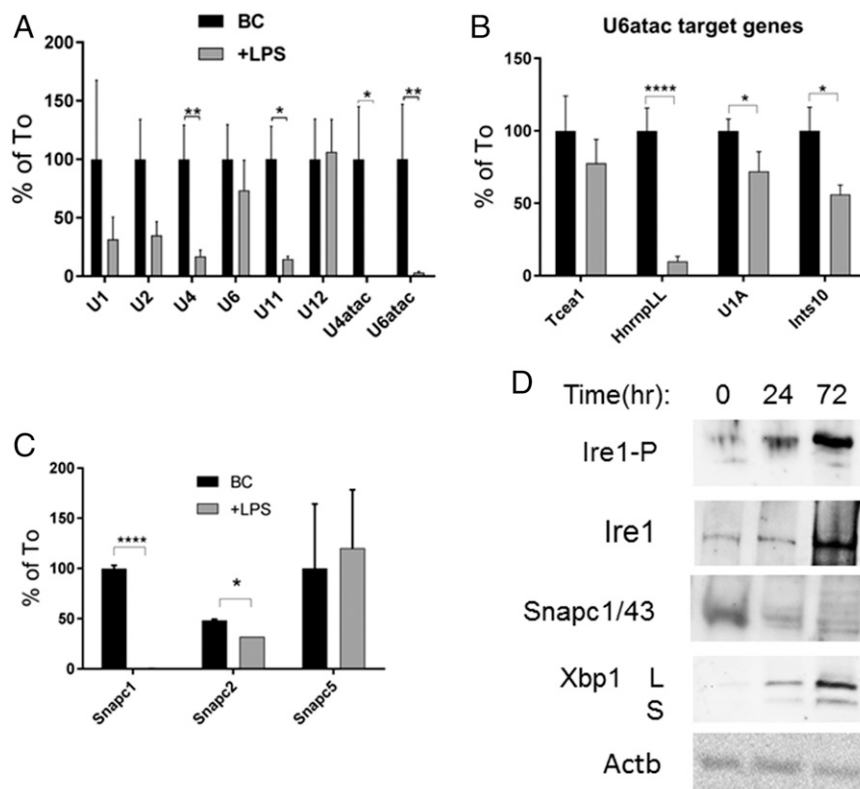
As shown in the pathway analyses (Fig. 7C), RNAs in 15 cell cycle pathways are altered in 18 h after LPS with immune signaling and metabolism represented by nine and six pathways, respectively. There are several pathways in the alternative splicing and mRNA processing pathways induced early after LPS. Addition of 4u8C and LPS modifies not only the number of genes

alternatively spliced but also the pathways in which those genes map. The time line of the changes we found is indicated in Fig. 8. Thus, we conclude that the Ire1-P pathway and RIDD have profound effects on the differentiation of the B cell into an ASC.

Discussion

We have shown that large changes in mRNA splicing occur in the B to ASC transition. In Fig. 8, we summarized the many factors that may contribute to the large number of changes in splicing seen, including ELL2 upregulation and ER stress. Although genes that get induced to higher levels in one stage or another have been the focus of many studies, it is important to realize that some genes have mRNAs that do not increase in abundance, and yet they can show alternative splicing. Many of these changes may be missed in flow cytometry and standard Western blotting using Abs that recognize only one exon. The genome project found that most multiexon genes can produce four to five different splicing products. Not all of these changes result in different proteins, yet many do. In our array studies, we have seen examples of such genes that have been documented in the literature to result in proteins with different amino or carboxyl termini, altered cellular location, or altered translation based on inclusion of alternative exons. We see splicing changes in exons in which the differences are 3-fold or

FIGURE 5. snRNAs decrease after LPS stimulation. **(A)** QPCR was performed with snRNA primers on random-primed cDNA from either ELL2^{+/+} B cells (BC) or from ELL2^{+/+} cells stimulated with LPS for 72 h (+LPS). The amount of PCR product was normalized relative to the determination of Hprt mRNA in the same sample on the same PCR plate. The amount of product in the BC sample was set to 100%, and the amount of product +LPS was calculated as a percentage so that the data could be presented succinctly on one graph. A minimum of three independent biological replicates was used, and QPCRs were performed at least three times at each time point for each snRNA. **(B)** Primers for the indicated mRNAs were used to determine the amount of each mRNA in BC and +LPS samples. Results are plotted as percentage of time zero and performed multiple times as described in (A). **(C)** Primers for the SnapC subunits were used in RT-QPCR and plotted and performed multiple times as described in (A). **(D)** Western blot of protein samples from BC or cells treated for 24 or 72 h with LPS. SnapC1 mRNA encodes a 43 kDa protein. Xbp1 long and short forms are indicated. Actin was used as a loading control. This represents one sample of the representative data from among three independent biological replicates. **p* < 0.05, ***p* < 0.01, *****p* < 0.0001.



more in *Hadc9*, *Ptbp3*, *MyD88*, and, not illustrated, *Traf7*, *Zbtb20*, *DNAjb6* (*hsp40*), *IL-2R* γ -chain, *Ppp2r5c*, *Srsf1*, *Ikzf1*, *Cmp1* (*c-maf*), *Elmo*, *Ugp2*, *Picalm*, *Tmem209*, *Hspa4* (*hsp70*), *Mapk1*, *Xiap*, *Eifak3*, *Cstf3*, and *Srpk2*, listed in order of descending splicing indexes. These genes fall in many pathways and it will be important for future research to determine the relevance of these changes in gene expression to the development of ASCs.

We show in this article that ELL2 has a widespread influence on gene expression beyond the IgH gene. We found changes in the splicing of many genes both between B cells and ASCs in ELL2-sufficient mice and between cells that are ELL2 sufficient versus deficient, which were especially pronounced in the mutually exclusive exon category. ELL2 induction causes increased expression of most of the ASC signature genes, *Irf4*, *Prdm1*, *Pou2af2*, and *Xbp1* mRNAs, all previously shown to influence gene expression to ASCs, and many of which bind ELL2 in our ChIP-seq studies. But many more genes in toto (5115) undergo alternative splicing without changes in abundance when ELL2 is induced, and the

number of splicing changes per gene are more numerous with ELL2 present. When we performed an overlap analysis as shown in the Venn diagram (Fig. 3C), we saw that in ~55% of the genes, splicing events are dependent on the presence of ELL2.

Of the 1039 genes with increased mRNA levels after the transition from B cells to ASCs at 72 h after LPS in ELL2-sufficient cells, 188 were V regions genes. Out of the remaining 851 non-V region genes, 635 showed changes in splicing both between B cells and ASC in ELL2^{+/+} mice and between ELL2^{+/+} and ELL2 cKO mice (Supplemental Table II). Only some of those were on the list of 2000 strong ChIP targets for ELL2 (see NCBI GEO list) (35). Therefore, we conclude that some mRNAs are influenced straightforwardly by ELL2 binding to their gene. Some are induced in the presence of ELL2 indirectly or fall below the strict cutoff of 10 tags per gene that we imposed.

We did a pathway analysis on the 343 genes that are induced by 72 h of LPS treatment when ELL2 is present and that are also differentially spliced between B cells and the ASCs. These genes

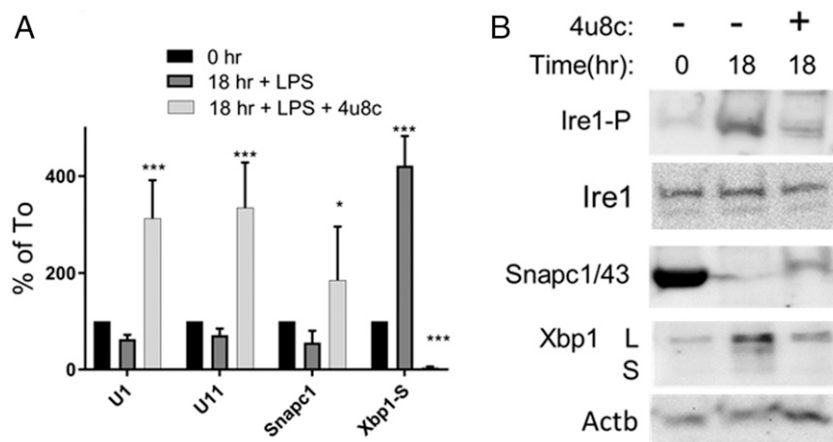


FIGURE 6. Loss of snRNA occurs early with ER stress. **(A)** QPCR was performed on RNA isolated from ELL2^{+/+} B cells (0 h), cells treated for 18 h plus LPS with or without 4u8C, an inhibitor of Ire1 phosphorylation, and the RIDD activity. Non-canonical Xbp1 splicing to the short form (Xbp1-S) as indicated. Three independent biological replicates were assay in triplicate. **(B)** Western blot of protein levels from B cells or cells treated for 18 h plus LPS with or without 4u8C. SnapC1 mRNA encodes a 43 kDa protein. Xbp1 long and short forms are indicated. Actin was used as a loading control. Representative of three independent biological replicates. **p* < 0.05, ***p* < 0.01, ****p* < 0.001.

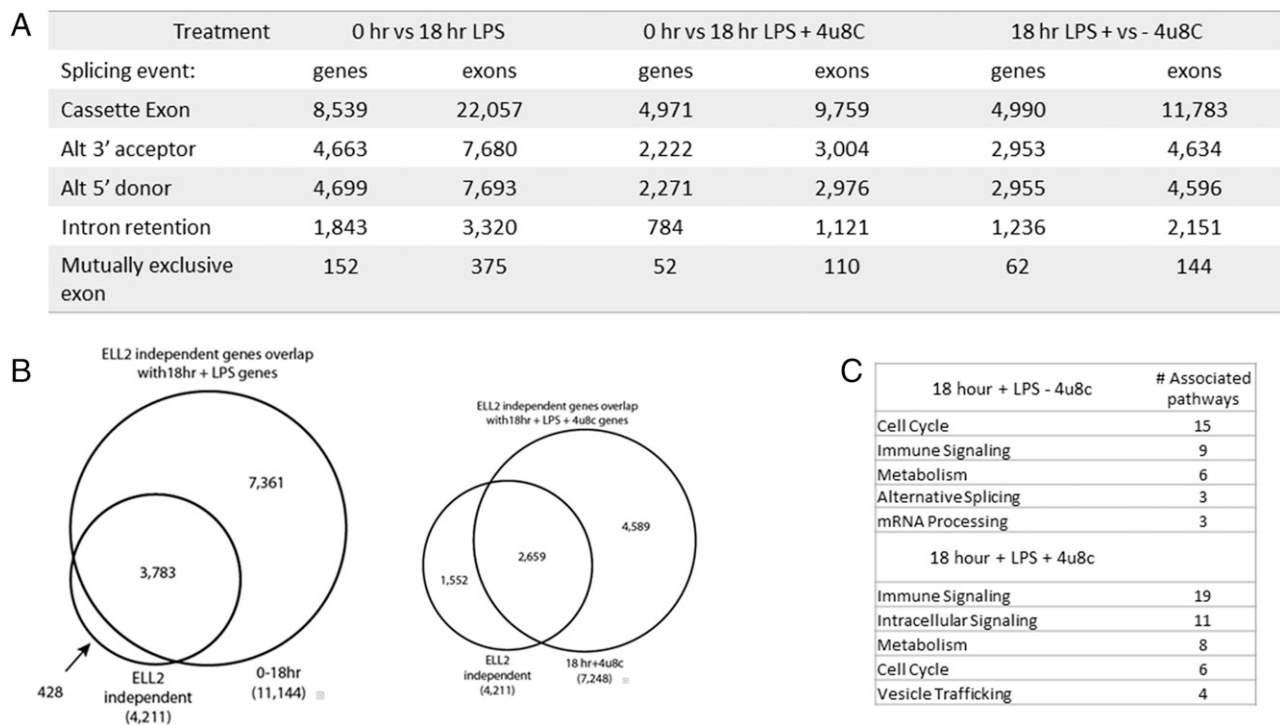


FIGURE 7. ER stress influences splicing patterns. **(A)** TAC software generated classifiers for differentially spliced events, broken down by number of genes and number of exons. Two-way comparison of each of the three 4u8c conditions (0 h, 18 h plus 4u8c, and 18 h minus 4u8c). Results determined with three independent biological replicates for the array data, see *Materials and Methods*. **(B)** Overlap between alternatively spliced genes in the ELL2-independent genes (genes differentially spliced in LPS-stimulated ELL2^{-/-} versus ELL2^{+/+}) and plus and minus 4u8c at 18 h after stimulation. **(C)** Tally of pathway analyses of alternatively spliced genes mined from the 18 h plus LPS minus 4u8c dataset (significance *p* value cutoff at *p* = 1 × 10⁻⁹) and the 18 h plus LPS plus 4u8c dataset (significance *p* value cutoff at *p* = 1 × 10⁻⁵).

are primarily associated with the cell cycle, N-glycan synthesis and processing, immune signaling, Golgi associated, and ER protein processing genes. A number of the genes in which ELL2 deficiency influences splicing show extended 5' UTRs. This phenomena of extended 5' UTRs was observed in meiotic differentiation in budding yeast in which these RNAs were poorly translated (30). This is yet another way in which mRNA sequence could influence the resulting protein products aside from overt changes in coding regions by alternative exon use.

Genome-wide association studies of altered IgG N-glycosylation phenotypes uncovered ELL2 as a significant gene for IgG glycosylation in humans (39), consistent with the results we found in our study. ELL2 is lacking in certain kinds of nonsecreting multiple myelomas (40), and an analysis of 505 patients with an ELL2 deficiency revealed decreased expression of mRNAs for Bip and Atf6 in the UPR pathway and decreased Pou2af1 and ELL1 (41), all of which we see here in the ELL2-altered pathways, either directly or indirectly. Pou2af1 is especially interesting because the gene is found associated with ELL2 by ChIP-seq and it encodes a protein that binds to Oct1 and Oct2 to stimulate transcription of genes that have the octamer sequence associated (42).

At 18 h after LPS stimulation, many genes are being alternatively spliced relative to the B cells at 0 h, more than the number seen at 72 h when the ASCs are focused on the task of Ig production and export. Many of these 18 h genes are involved in cell division and immune signaling pathways. Ninety percent of the genes that are alternatively spliced independently of ELL2 in the 72 h plus LPS samples overlap with 0–18 h alternatively spliced genes. Because ELL2 is not significantly upregulated until more than 24 h after LPS, this is understandable.

The number of genes scored as alternatively spliced 0 h versus 18 h after LPS represents a combination of newly synthesized

mRNAs made after LPS, loss of some 0 h RNAs by the RIDD process, and persistence of the previously made, undegraded, B cell mRNAs. When the ER phosphorylation of Ire1 is blocked by 4u8C, the number of genes displaying alternative splicing events in all categories relative to B cells is decreased. The RNAs in 0 versus 18 h plus 4u8C show fewer cell cycle genes but an increase in immune system signaling and intracellular signaling pathways. Noncanonical splicing of Xbp1 to the short form is inhibited in 4u8C. Because it is the short form of Xbp1 that encodes a transcription factor causing induction of the UPR genes, these genes would not be turned on in the presence of 4u8C and thus they would be underrepresented. The levels of the snRNAs rise in 4u8C, which could be expected to perturb splicing patterns. Comparing genes that are expressed both plus and minus 4u8C, >4990 cassette exon splicing changes and changes in all the other categories occur. Ire1 phosphorylation appears to have a large effect on alternative splicing patterns, some of it perhaps through changes in the levels of the RNAs in the snRNA pathway.

RIDD appears to require both Ire1-P activity and ER stress (43). Under severe stress, Ire1-mediated RNA decay can even promote apoptosis (44). Through RIDD, selective mRNA decay is able to alleviate some of the stress on the ER and presumably make space for the massive upregulation of UPR proteins and their mRNAs (43); this may then contribute to the diversity of the splicing pattern of the RNAs that survive at 18 h because RIDD inhibition reduces diversity of alternatively spliced products.

We have shown that changing the splicing pattern of RNAs in the B to ASC transition is a complex process that depends on induction of ELL2 and may require Ire1-phosphorylation and RIDD. ELL2 may act with either direct binding to genes or indirect effects on their expression. Clearly, more work needs to be done to understand

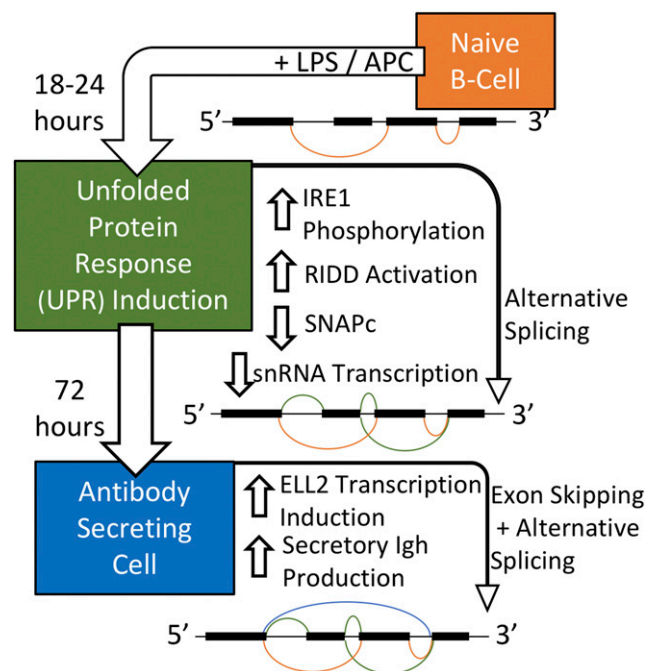


FIGURE 8. Summary. Data presented in this work are summarized in a time line depicting alternative splicing at 18 and 72 h after LPS treatment and the potential influences on it. The exon splicing patterns are figuratively meant to show increasing complexity with time. We hypothesize that SnapC and snRNA decreases may be linked to the RIDD activity induced by ER stress, although this is speculative at this point.

the interplay of all of these factors and the effect of the changing levels of the snRNAs which may contribute.

Disclosures

The authors have no financial conflicts of interest.

References

- Johnson, J. M., J. Castle, P. Garrett-Engele, Z. Kan, P. M. Loerch, C. D. Armour, R. Santos, E. E. Schadt, R. Stoughton, and D. D. Shoemaker. 2003. Genome-wide survey of human alternative pre-mRNA splicing with exon junction microarrays. *Science* 302: 2141–2144.
- Rozen, S., A. Tieri, G. Ridner, A.-K. Stark, T. Schmalzer, G. Ben-Nissan, W. Dubiel, and M. Sharon. 2013. Exposing the subunit diversity within protein complexes: a mass spectrometry approach. *Methods* 59: 270–277.
- Shi, W., Y. Liao, S. N. Willis, N. Taubenheim, M. Inouye, D. M. Tarlinton, G. K. Smyth, P. D. Hodgkin, S. L. Nutt, and L. M. Corcoran. 2015. Transcriptional profiling of mouse B cell terminal differentiation defines a signature for antibody-secreting plasma cells. *Nat. Immunol.* 16: 663–673.
- Bayles, I., and C. Milcarek. 2014. Plasma cell formation, secretion, and persistence: the short and the long of it. *Crit. Rev. Immunol.* 34: 481–499.
- Peterson, M. L. 2007. Mechanisms controlling production of membrane and secreted immunoglobulin during B cell development. *Immunol. Res.* 37: 33–46.
- Ma, J., S. I. Gunderson, and C. Phillips. 2006. Non-snRNP U1A levels decrease during mammalian B-cell differentiation and release the IgM secretory poly(A) site from repression. *RNA* 12: 122–132.
- Shell, S. A., K. Martincic, J. Tran, and C. Milcarek. 2007. Increased phosphorylation of the carboxyl-terminal domain of RNA polymerase II and loading of polyadenylation and cotranscriptional factors contribute to regulation of the Ig heavy chain mRNA in plasma cells. *J. Immunol.* 179: 7663–7673.
- Milcarek, C., M. Albring, C. Langer, and K. S. Park. 2011. The eleven-nineteen lysine-rich leukemia gene (ELL2) influences the histone H3 protein modifications accompanying the shift to secretory immunoglobulin heavy chain mRNA production. *J. Biol. Chem.* 286: 33795–33803.
- Park, K. S., I. Bayles, A. Szlachta-McGinn, J. Paul, J. Boiko, P. Santos, J. Liu, Z. Wang, L. Borghesi, and C. Milcarek. 2014. Transcription elongation factor ELL2 drives Ig secretory-specific mRNA production and the unfolded protein response. *J. Immunol.* 193: 4663–4674.
- Martincic, K., S. A. Alkan, A. Cheate, L. Borghesi, and C. Milcarek. 2009. Transcription elongation factor ELL2 directs immunoglobulin secretion in plasma cells by stimulating altered RNA processing. *Nat. Immunol.* 10: 1102–1109.

- Nelson, A. M., and C. Milcarek. 2017. Transcription elongation factor ELL2 in antibody secreting cells, myeloma, and HIV infection: a full measure of activity. *Curr. Trends Immunol.* 18: 1–11.
- Milcarek, C., K. Martincic, L.-H. Chung-Ganster, and C. S. Lutz. 2003. The snRNP-associated U1A levels change following IL-6 stimulation of human B-cells. *Mol. Immunol.* 39: 809–814.
- Ray, R., K. Ray, and C. K. Panda. 1997. Differential alterations in metabolic pattern of the six major UsnRNAs during development. *Mol. Cell. Biochem.* 177: 79–88.
- Cheng, Z., Z. Du, Y. Shang, Y. Zhang, and T. Zhang. 2017. A preliminary study: PS1 increases U1 snRNA expression associated with AD. *J. Mol. Neurosci.* 62: 269–275.
- Singh, R. K., and T. A. Cooper. 2012. Pre-mRNA splicing in disease and therapeutics. *Trends Mol. Med.* 18: 472–482.
- Aragon, I. V., R. A. Barrington, S. Jackowski, K. Mori, and J. W. Brewer. 2012. The specialized unfolded protein response of B lymphocytes: ATF6 α -independent development of antibody-secreting B cells. *Mol. Immunol.* 51: 347–355.
- Aronov, M., and B. Tirosh. 2016. Metabolic control of plasma cell differentiation- what we know and what we don't know. *J. Clin. Immunol.* 36(Suppl. 1): 12–17.
- Kumazaki, K., B. Tirosh, R. Maehr, M. Boes, T. Honjo, and H. L. Ploegh. 2007. AID-/- mice are agammaglobulinemic and fail to maintain B220-CD138+ plasma cells. *J. Immunol.* 178: 2192–2203.
- Tirasophon, W., K. Lee, B. Callaghan, A. Welihinda, and R. J. Kaufman. 2000. The endoribonuclease activity of mammalian IRE1 autoregulates its mRNA and is required for the unfolded protein response. *Genes Dev.* 14: 2725–2736.
- So, J.-S., K. Y. Hur, M. Tarrio, V. Ruda, M. Frank-Kamenetsky, K. Fitzgerald, V. Koteliensky, A. H. Lichtman, T. Iwawaki, L. H. Glimcher, and A.-H. Lee. 2012. Silencing of lipid metabolism genes through IRE1 α -mediated mRNA decay lowers plasma lipids in mice. *Cell Metab.* 16: 487–499.
- Cross, B. C. S., P. J. Bond, P. G. Sadowski, B. K. Jha, J. Zak, J. M. Goodman, R. H. Silverman, T. A. Neubert, I. R. Baxendale, D. Ron, and H. P. Harding. 2012. The molecular basis for selective inhibition of unconventional mRNA splicing by an IRE1-binding small molecule. *Proc. Natl. Acad. Sci. USA* 109: E869–E878.
- Genovese, C., and C. Milcarek. 1990. Increased half-life of mu immunoglobulin mRNA during mouse B cell development increases its abundance. *Mol. Immunol.* 27: 733–743.
- Genovese, C., S. Harrold, and C. Milcarek. 1991. Differential mRNA stabilities affect mRNA levels in mutant mouse myeloma cells. *Somat. Cell Mol. Genet.* 17: 69–81.
- Petrie, K., F. Guidez, L. Howell, L. Healy, S. Waxman, M. Greaves, and A. Zelen. 2003. The histone deacetylase 9 gene encodes multiple protein isoforms. *J. Biol. Chem.* 278: 16059–16072.
- Tan, L.-Y., P. Whitfield, M. Llorian, E. Monzon-Casanova, M. D. Diaz-Munoz, M. Turner, and C. W. J. Smith. 2015. Generation of functionally distinct isoforms of PTBP3 by alternative splicing and translation initiation. *Nucleic Acids Res.* 43: 5586–5600.
- De Arras, L., and S. Alper. 2013. Limiting of the innate immune response by SF3A-dependent control of MyD88 alternative mRNA splicing. *PLoS Genet.* 9: e1003855.
- Janssens, S., K. Burns, J. Tschopp, and R. Beyaert. 2002. Regulation of interleukin-1 and lipopolysaccharide-induced NF- κ B activation by alternative splicing of MyD88. *Curr. Biol.* 12: 467–471.
- de la Mata, M., C. R. Alonso, S. Kadener, J. P. Fededa, M. Blaustein, F. Pelisch, P. Cramer, D. Bentley, and A. R. Kornblith. 2003. A slow RNA polymerase II affects alternative splicing *in vivo*. *Mol. Cell* 12: 525–532.
- Martincic, K., R. Campbell, G. Edwards-Gilbert, L. Souan, M. T. Lotze, and C. Milcarek. 1998. Increase in the 64-kDa subunit of the polyadenylation/cleavage stimulatory factor during the G0 to S phase transition. *Proc. Natl. Acad. Sci. USA* 95: 11095–11100.
- Cheng, Z., G. M. Otto, E. N. Powers, A. Keskin, P. Mertins, S. A. Carr, M. Jovanovic, and G. A. Brar. 2018. Pervasive, coordinated protein-level changes driven by transcript isoform switching during meiosis. *Cell* 172: 910–923.e16.
- Smith, E., C. Lin, and A. Shilatifard. 2011. The super elongation complex (SEC) and MLL in development and disease. *Genes Dev.* 25: 661–672.
- Listerman, I., A. S. Bledau, I. Grishina, and K. M. Neugebauer. 2007. Extragenic accumulation of RNA polymerase II enhances transcription by RNA polymerase III. *PLoS Genet* 3: e212.
- Underhill, G. H., D. George, E. G. Bremer, and G. S. Kansas. 2003. Gene expression profiling reveals a highly specialized genetic program of plasma cells. *Blood* 101: 4013–4021.
- Underhill, G. H., K. P. Kolli, and G. S. Kansas. 2003. Complexity within the plasma cell compartment of mice deficient in both E- and P-selectin: implications for plasma cell differentiation. *Blood* 102: 4076–4083.
- Baumgartner, M., C. Lemoine, S. Al Seesi, D. K. P. Karunakaran, N. Sturrock, A. R. Banday, A. M. Kilcollins, I. Mandoiu, and R. N. Kanadia. 2015. Minor splicing snRNAs are enriched in the developing mouse CNS and are crucial for survival of differentiating retinal neurons. *Dev. Neurobiol.* 75: 895–907.
- Murphy, S., J. B. Yoon, T. Gerster, and R. G. Roeder. 1992. Oct-1 and Oct-2 potentiate functional interactions of a transcription factor with the proximal sequence element of small nuclear RNA genes. *Mol. Cell. Biol.* 12: 3247–3261.
- Henry, R. W., V. Mittal, B. Ma, R. Kobayashi, and N. Hernandez. 1998. SNAP19 mediates the assembly of a functional core promoter complex (SNAPc) shared by RNA polymerases II and III. *Genes Dev.* 12: 2664–2672.

38. Smith, E. R., C. Lin, A. S. Garrett, J. Thornton, N. Mohaghegh, D. Hu, J. Jackson, A. Saraf, S. K. Swanson, C. Seidel, et al. 2011. The little elongation complex regulates small nuclear RNA transcription. *Mol. Cell* 44: 954–965.
39. Shen, X., L. Klarić, S. Sharapov, M. Mangino, Z. Ning, D. Wu, I. Trbojević-Akmačić, M. Pučić-Baković, I. Rudan, O. Polašek, et al. 2017. Multivariate discovery and replication of five novel loci associated with immunoglobulin G N-glycosylation. *Nat. Commun.* 8: 447.
40. Swaminathan, B., G. Thorleifsson, M. Jöud, M. Ali, E. Johnsson, R. Ajore, P. Sulem, B.-M. Halvarsson, G. Eyjolfsson, V. Haraldsdottir, et al. 2015. Variants in ELL2 influencing immunoglobulin levels associate with multiple myeloma. *Nat. Commun.* 6: 7213.
41. Li, N., D. C. Johnson, N. Weinhold, S. Kimber, S. E. Dobbins, J. S. Mitchell, B. Kinnersley, A. Sud, P. J. Law, G. Orlando, et al. 2017. Genetic predisposition to multiple myeloma at 5q15 is mediated by an ELL2 enhancer polymorphism. *Cell Rep.* 20: 2556–2564.
42. Greiner, A., K. B. Müller, J. Hess, K. Pfeffer, H. K. Müller-Hermelink, and T. Wirth. 2000. Up-regulation of BOB.1/OBF.1 expression in normal germinal center B cells and germinal center-derived lymphomas. *Am. J. Pathol.* 156: 501–507.
43. Hollien, J., J. H. Lin, H. Li, N. Stevens, P. Walter, and J. S. Weissman. 2009. Regulated Ire1-dependent decay of messenger RNAs in mammalian cells. *J. Cell Biol.* 186: 323–331.
44. Han, D., A. G. Lerner, L. Vande Walle, J. P. Upton, W. Xu, A. Hagen, B. J. Backes, S. A. Oakes, and F. R. Papa. 2009. IRE1alpha kinase activation modes control alternate endoribonuclease outputs to determine divergent cell fates. *Cell* 138: 562–575.